Monodisperse silica nanoparticles encapsulating upconversion fluorescent and superparamagnetic nanocrystals†

Zhaoyang Liu,* Guangshun Yi, Haitao Zhang, Jun Ding, Yongwei Zhang and Junmin Xue*

Received (in Cambridge, UK) 8th October 2007, Accepted 22nd November 2007
First published as an Advance Article on the web 4th December 2007
DOI: 10.1039/b715402j

A new type of multifunctional silica-coated nanocomposites, detectable by their upconversion fluorescence and addressable by a magnetic field, was synthesized.

To find an appropriate nanosized fluorescent label remains a challenging task and is crucial to the development of modern biomedical sciences. Conventional downconversion fluorescent labels, such as quantum dots (QDs), which require a higher-energy wavelength to be excited, emit one lower-energy photon after absorbing a UV or visible photon.[1,2] The biomedical utility of these single-photon fluorescent labels has been limited due to their inherent toxicity, chemical instability, low light-penetration depth, possible severe photodamage to living organisms and low signal-to-noise ratio as a fact that many biological samples show autofluorescence excited by short-wavelength UV radiation. Upconversion fluorescent nanocrystals (UCs), which are excited in the near infrared region instead of the UV region to give emission in the visible domain, can be a good alternative.[3–5] These upconversion nanocrystals emit one photon in the visible region after absorbing two or more near-infrared (NIR) photons. Various emission colors of visible light can be achieved from upconversion materials under the NIR excitation.[4] In comparison with down-conversion fluorescent nanocrystals, UCs show a higher chemical stability, higher quantum yields, lower toxicity, lower background light due to the absence of autofluorescence, and minimal photodamage to biological tissues due to the noninvasive NIR excitation light. In addition, the NIR excitation laser is compact, high-power, and inexpensive. All these favorable properties have indicated the great potential of UCs in the analysis of biological samples, especially for fluorescent imaging *in vivo*.[6] Among the upconversion fluorescent materials, $NaYF_4$:Yb, Er(Tm) nanocrystals are the most efficient NIR-to-visible upconversion phosphors.[7] In a previous effort, we successfully synthesized hexagonal $NaYF_4$:Yb,Er(Tm) nanocrystals with particle size as small as 10 nm and remarkable upconversion fluorescence.[8]

Superparamagnetic nanoparticles (SPMs) have been widely studied because of their potential applications in biomedical fields such as biomolecular separation, target-drug delivery, cancer diagnosis and treatment, DNA separation and detection sequencing of oligonucleotides, and magnetic resonance imaging (MRI).[9–11] Among superparamagnetic particles, magnetite (Fe_3O_4) and maghemite (γ-Fe_2O_3) nanocrystals have been of great interest not only for the study of fundamental magnetic properties, but also for biomedical applications.

For all the biomedical applications mentioned above, both the fluorescent and superparamagnetic nanoparticles would be required to be uniform in size, chemically stable, and well dispersed in aqueous media. It has been demonstrated that the formation of an inert silica coating on the surfaces of nanoparticles could help prevent their aggregation in liquid and improve their chemical stability.[12] Another advantage of the silica shell is that the silica surface is often terminated by a silanol group which can react with various coupling agents to covalently attach specific ligands to the surfaces of these nanoparticles. Such a capability will open the door to the design and synthesis of nanoparticles that can be used to deliver specific ligands to target organs *via* the antibody–antigen recognition.[13]

In this communication, a new type of monodisperse core/shell nanoparticles with both upconversion fluorescent nanocrystals and superparamagnetic nanocrystals encapsulated in silica shells (SiO_2/UC-SPM) was synthesized. The obtained composite nanoparticles are capable of emitting pure eye-visible fluorescence upon NIR excitation and being driven by an external magnetic field to a specific target, which make them attractive for a variety of biomedical applications, such as bioimaging, drug targeting and bioseparation.

The SiO_2/UC-SPM nanoparticles were synthesized by using a simple reverse-microemulsion method. As-prepared 10 nm $NaYF_4$:20%Yb,2%Er UCs and 16 nm Fe_3O_4 SPMs[14] were first synthesized separately (see ESI†), prior to their introduction to the reverse microemulsion system for silica coating. Typically, Triton X-100 (*tert*-octylphenoxypolyoxyethylene) and octanol were dissolved in cyclohexane by sonication. Next, cyclohexane solutions of $NaYF_4$:Yb,Er UCs and Fe_3O_4 SPMs were added. The resulting mixture was stirred, and ammonium hydroxide was added to form a brown solution of the reverse microemulsion. Finally, TEOS (tetraethyl orthosilicate) and APS (aminopropyltriethoxysilane) were added, the formation of silica coating was initiated by hydrolyzing TEOS and APS, catalyzed by ammonia.[12,13] The reaction was continued for 24 h. The resulting SiO_2/UC-SPM composite nanoparticles were collected by a magnet or centrifuging, washed, and redispersed in ethanol or deionized water.

An FE-SEM image (Fig. 1(a)) of SiO_2/UC-SPM nanoparticles revealed that the silica particles are quite uniform in size with an average particle diameter of around 60 nm, which is within the applicable size range for drug and gene delivery applications.[15,16] TEM and HRTEM images of SiO_2/UC-SPM nanoparticles are

Department of Materials Science and Engineering, National University of Singapore, Singapore, 117576, Republic of Singapore.
E-mail: mselz@nus.edu.sg; msexuejm@nus.edu.sg; Fax: 65-67763604; Tel: 65-65164655

† Electronic supplementary information (ESI) available: Details of preparation techniques and characterizations with TEM and magnetic measurement. See DOI: 10.1039/b715402j

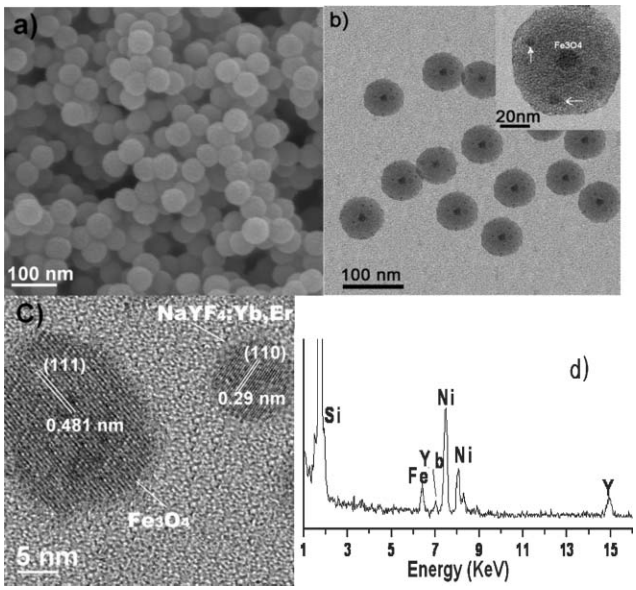

Fig. 1 FE-SEM (a) and TEM (b) images of silica nanoparticles encapsulating upconversion fluorescent nanocrystals (UCs) and superparamagnetic nanocrystals (SPMs). The inset in (b) is the higher-magnification image of a typical SiO_2/UC-SPM nanoparticle: note the presence of both Fe_3O_4 SPMs (larger crystallites) and UCs (finer crystallites denoted by arrows). (c) High-resolution TEM image of the SiO_2/UC-SPM nanoparticles. (d) EDX data of SiO_2/UC-SPM nanoparticles, showing the components (Yb and Y from $NaYF_4$:Yb,Er, Fe from Fe_3O_4, and Si from SiO_2, Ni from TEM Ni grid).

presented in Fig. 1(b) and (c), respectively. The TEM image shows that the silica core shell nanostructure has been successfully formed. The inset in Fig. 1(b) is a higher-magnification image of a typical SiO_2/UC-SPM nanoparticle, showing the presence of both Fe_3O_4 SPMs (larger crystallites) and UCs (finer crystallites denoted by arrows). The presence of both $NaYF_4$:Yb,Er and Fe_3O_4 nanoparticles embedded in silica nanoparticles is further confirmed by the HRTEM image shown in Fig. 1(c). The interplanar spacings of 0.481 and 0.29 nm correspond to the (111) crystal plane of Fe_3O_4 and (110) crystal plane of $NaYF_4$:Yb,Er, respectively.[8,14] A higher-magnification TEM image of the SiO_2/UC-SPM nanoparticles is shown in Fig. SI2, ESI,† which indicates that the number ratio between the small ($NaYF_4$:Yb,Er) and large (Fe_3O_4) particles is roughly 3 : 1. The nanocrystals are dispersed well in the composite core–shell structures. Energy-dispersive X-ray (EDX) analysis of SiO_2/UC-SPM nanoparticles confirmed the presence of all elements that were expected: Yb and Y from $NaYF_4$:Yb,Er, Fe from Fe_3O_4, and Si from SiO_2, indicating that both UCs and SPMs were successfully encapsulated in the silica nanoparticles (Fig. 1(d)).

The upconversion fluorescent material we used was Yb^{3+}/Er^{3+} ion-pair doped hexagonal $NaYF_4$ nanocrystals. To the best of our knowledge, the hexagonal phase $NaYF_4$ is reported as one of the most efficient hosts for performing infrared to visible photon conversion when activated by Yb^{3+}/Er^{3+} ion-pairs.[8] Fig. 2(a) shows the room-temperature upconversion fluorescence spectra of the SiO_2/UC-SPM nanoparticles under 980 nm NIR excitation. There were three emission peaks at 522.5, 541.5 and 655.5 nm, which are assigned to the $^4H_{11/2}$–$^4I_{15/2}$, $^4S_{3/2}$–$^4I_{15/2}$ and $^4F_{9/2}$–$^4I_{15/2}$

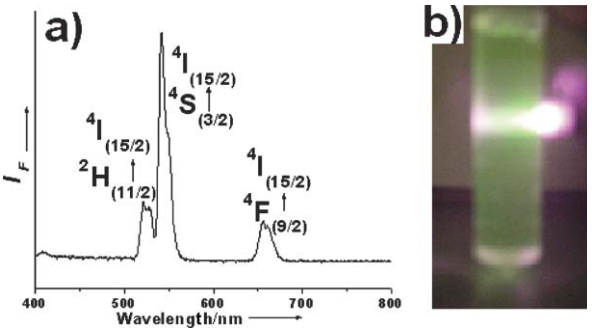

Fig. 2 (a) Room-temperature upconversion fluorescence spectra of SiO_2/UC-SPM nanoparticles under 980 nm NIR excitation. (b) Photograph of the upconversion fluorescence (green) of SiO_2/UC-SPM nanoparticles in aqueous solutions.

transitions of Er^{3+}, respectively.[6,8] It is worth noting that the green emission (at 541.5 nm) is the main peak, while the other peaks are very weak in comparison. An ideal probe should emit at spectrally resolvable energies with a narrow, symmetric emission spectrum.[2] Here, the composite nanoparticles emit strong and pure green fluorescence with a symmetric and narrow emission spectrum upon excitation at a single wavelength (980-nm laser), which makes them suitable as a bioprobe. The strong green UC fluorescence from suspensions of the SiO_2/UC-SPM nanoparticles in water upon excitation with a 980-nm laser is easily visible to the naked eye (Fig. 2b).

Magnetic characterization was performed using a superconducting quantum interference device (SQUID). These raw data were presented in electromagnetic units per gram of sample. Field-dependent magnetization plots illustrated that SiO_2/UC-SPM nanoparticles were superparamagnetic at 300 K (Fig. 3(a)) and ferromagnetic at 5 K (Fig. 3(a) inset). The composite nanoparticles reached a saturation moment of 1.64 emu g^{-1} at 300 K. As compared to the Fe_3O_4 nanocrystals, which show a saturation magnetization of 59 emu/g (as shown in Fig. SI3, ESI†), the saturation magnetization of the silica-coated nanoparticles (1.64 emu g^{-1}) is lower. The reduction in saturation magnetization value can be explained by taking into account the diamagnetic contribution of the silica shell surrounding the magnetic cores. Zero-field-cooled (ZFC) and field-cooled (FC) magnetization curves were obtained under an applied field of 100 Oe between 5

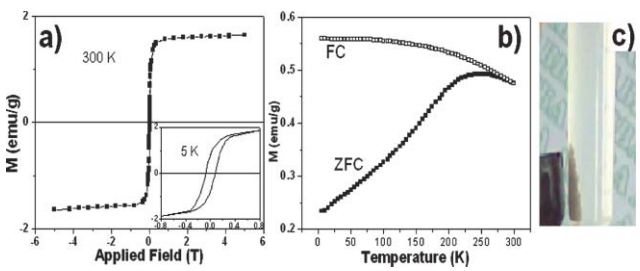

Fig. 3 Magnetic measurements of SiO_2/UC-SPM nanoparticles showing (a) magnetization–applied magnetic field (*M*–*H*) and (b) zero-field-cooled (ZFC) and field-cooled (FC) magnetization curves. The inset in (a) is a magnified view of the magnetization curves at low applied fields. (c) Photograph of SiO_2/UC-SPM nanoparticles driven by an external magnet (black).

and 300 K (Fig. 3(b)). Both curves coincide at high temperature and begin to separate as the temperature decreases. They exhibited the typical behavior of Fe_3O_4 nanoparticles. Such behavior is characteristic of superparamagnetism[10] and is due to the progressive deblocking of particles as the temperature increases. The blocking temperature (T_B) is $\sim$240 K. Fig. 3(c) shows a photograph of an aqueous dispersion of the fluorescent/magnetic nanoparticles and illustrates the magnetic manipulation ability. When an external magnetic field is placed beside the glass vial, the composite nanoparticles can be directed near the magnet. These magnetic properties will allow the nanoparticles to be used in biomedical applications since they undergo strong magnetization, allowing for efficient magnetic delivery and separation.

In summary, a unique silica core–shell structure containing superparamagnetic and upconversion fluorescent nanocrystals was successfully synthesized *via* an emulsion route. The obtained composite nanoparticles, which demonstrate both superparamagnetic and upconversion fluorescence properties, are promising candidate materials for applications of bioimaging, drug targeting and bioseparation.

The authors thank Dr Zhang Jixuan for TEM characterization. This work was supported by the Faculty of Engineering, National University of Singapore, WBS No: R-284-000-050-133.

Notes and references

1 W. J. M. Mulder, R. Koole, R. J. Brandwijk, G. Storm, P. T. K. Chin, G. J. Strijkers, C. M. Donega, K. Nicolay and A. W. Griffioen, *Nano Lett.*, 2006, **6**, 1.
2 E. Beaurepaire, V. Buissette, M. P. Sauviat, D. Giaume, K. Lahlil, A. Mercuri, D. Casanova, A. Huignard, J. L. Martin, T. Gacoin, J. P. Boilot and A. Alexandrou, *Nano Lett.*, 2004, **4**, 2079.
3 H. Sertchook and D. Avnir, *Chem. Mater.*, 2003, **15**, 1690.
4 F. Rijke, H. Zijlmans, S. Li, T. Vail, A. K. Raap, R. S. Niedbala and H. J. Tanke, *Nat. Biotechnol.*, 2001, **19**, 273.
5 G. S. Yi, H. C. Lu, S. Y. Zhao, G. Yue, W. J. Yang, D. P. Chen and L. H. Guo, *Nano Lett.*, 2004, **4**, 2191.
6 L. Y. Wang and Y. D. Li., *Chem. Commun.*, 2006, **24**, 2557.
7 Z. Q. Li and Y. Zhang, *Angew. Chem., Int. Ed.*, 2006, **45**, 7732.
8 G. S. Yi and G. M. Chow, *Adv. Funct. Mater.*, 2006, **16**, 2324.
9 Y. Lu, Y. D. Yin, B. T. Mayers and Y. N. Xia, *Nano Lett.*, 2002, **2**, 183.
10 V. Salgueiriño-Maceira, M. A. Correa-Duarte, M. Spasova, L. M. Liz-Marzán and M. Farle, *Adv. Funct. Mater.*, 2006, **16**, 509.
11 J. Kim, J. E. Lee, J. Lee, J. H. Yu, B. C. Kim, K. An, Y. Hwang, C. H. Shin, J. G. Park, J. Kim and T. Hyeon, *J. Am. Chem. Soc.*, 2006, **128**, 688.
12 Y. H. Yang and M. Y. Gao, *Adv. Mater.*, 2005, **17**, 2354.
13 D. K. Yi, S. T. Selvan, S. S. Lee, G. C. Papaefthymiou, D. Kundaliya and J. Y. Ying, *J. Am. Chem. Soc.*, 2005, **127**, 4990.
14 S. H. Sun and H. Zeng, *J. Am. Chem. Soc.*, 2002, **124**, 8204.
15 C. Y. Lai, B. G. Trewyn, D. M. Jeftinija, K. Jeftinija, S. Xu, S. Jeftinija and V. S. Y. Lin, *J. Am. Chem. Soc.*, 2003, **125**, 4451.
16 D. R. Radu, C. Y. Lai, K. Jeftinija, E. W. Rowe, S. Jeftinija and V. S. Y. Lin, *J. Am. Chem. Soc.*, 2004, **126**, 13216.

